

Numerical Simulation of Intermittently Controlled Multiple Impinging Jets

K. Tsujimoto¹, K. Jinno¹, T. Shakouchi¹ and T. Ando¹

¹Division of Mechanical Engineering, Graduate School of Engineering,
 Mie University, 1577 Kurimamachiya-cho, Tsu 514-8507, Japan

Abstract

A single impinging jet (SIJ) produces a high heat transfer rate around an impinging position on an impinging wall, while the heat transfer performance (HTP) decays increasing the distance from the impinging position. Thus in order to overcome the shortcoming of SIJ: the occurrence of both inhomogeneous heat distribution on the wall and the narrow heating area, multiple impinging jets (MIJ) are generally introduced. Thus far it is well-known that each jet of MIJ interacts with each other, producing the complex flow field, in addition, the HTP is significantly influenced by their interaction. In the present study, we conduct the DNS (direct numerical simulation) of two round impinging jets arranged at an inflow of flow field. In addition, we introduce the intermittent control for jets so as to reduce the interaction between each jet. As control parameters, both the period of intermittent control and the phase difference between the two jets are varied. From the time-averaged velocity distribution, it reveals that the generation of flow phenomena such as up-wash due to the interaction between two jets is reduced through the intermittent control and that the Nusselt number on the impinging plate is fairly improved than that of an uncontrolled case. In particular, it turns out that the total heat transfer on the impinging plate is improved under the longer period and large phase difference within the control parameter range.

Introduction

Impinging jet is widely used for cooling of industrial applications such as electric device, blades of gas turbines, hot steel and so on, since it possesses high performance of heat transfer rate and is easier to implement into various systems. Their characteristics are reviewed by a few notable literature[4, 11]: impinging jets are subdivided into three regions, such as free jet region, stagnation region, and wall jet region; the performance of heat transfer on the impinging wall is depending on the Reynolds number, the shape of nozzle, the number of nozzle, the distance between nozzle and impinging wall and so on. Further a single impinging jet produces a high heat transfer rate around an impinging position on impinging wall, while the heat transfer performance decays increasing distance from the impinging position. Thus in order to overcome the shortcoming of single impinging jets such as the occurrence of both inhomogeneous heat distribution on the wall and the narrow heating area, multiple impinging jets (MIJ) are generally introduced in industrial applications. Thus far for MIJ, it is well-known that each jet of MIJ interacts with each other, producing a complex flow field[2, 12]. In addition, the heat transfer performance is significantly influenced by their interaction. Therefore new control procedure of MIJ should be developed to improve the heat transfer performance.

Thus far, since pulsating or intermittently issuing jet is expected to be capable of inducing higher turbulent mixing and successively enhancing heat transfer, the possibility of this control method is experimentally and numerically examined. At the state of the art, some useful characteristics concerning SIJ (single impinging jet) have been reported in literature[6, 9, 3, 13]. Further to improve heat transfer and uniformity of heat trans-

fer on impinging wall of MIJ[14, 7, 1], plane or slot jets were mainly targeted and not experimentally but numerically examined using RANS, on the other hand, MIJ consisting of round jets are not well investigated.

In the present study, in order to enhance heat transfer on the impinging wall, we propose a control method in which an intermittent round impinging jet is arranged at an inflow of flow field. As control parameters, both the period of intermittent control and the phase difference between the two jets are varied. Further to high accurately predict the heat transfer performance of the proposed method, we conduct DNS in which sine or cosine series and 6th order compact scheme are assembled, and a fringe technique[8] is used to realize a surrounding boundary condition. From the view of time-averaged physical quantities, it reveals that the flow phenomena such as up-wash due to the interaction between two jets is reduced through the intermittent control, and that the Nusselt number on the impinging plate is fairly improved than that of the uncontrolled case.

Numerical Method

Governing Equations and Discretization

Under the assumption of incompressible flow, the governing equations are as follows :

$$\frac{\partial u_i}{\partial x_i} = 0 \quad (1)$$

$$\frac{\partial u_i}{\partial t} + h_i = -\frac{1}{\rho} \frac{\partial p}{\partial x_i} + \frac{1}{Re} \frac{\partial^2 u_i}{\partial x_j \partial x_j} \quad (2)$$

$$(h_i = \varepsilon_{ijk} \omega_j u_k, \omega_j : \text{vorticity})$$

$$\frac{\partial T}{\partial t} + u_i \frac{\partial T}{\partial x_i} = \frac{1}{RePr} \frac{\partial^2 T}{\partial x_i \partial x_i} \quad (3)$$

where u_i is velocity component, p is total pressure, T is temperature and ε_{ijk} is Levi-Civita symbol. The convective terms of equation (2) are described as rotational form. Above equations are normalized by both the diameter of the inlet jet, D and the inlet velocity, V_0 . Reynold number and Prandtl number are defined as $Re = V_0 D / \nu$ (ν : dynamic viscosity) and $Pr = \nu / \alpha$ (α : thermal conductivity), respectively.

Figure 1 shows the computational volume and coordinate systems. The computational volume is a rectangular box. The origin of axes is set at the center of two jets. The wall-normal direction, y and two horizontal directions, x, z are set, and the velocity component for each direction denotes u, v and w , respectively. The spatial discretization is performed with sine or cosine series expansion in x and z directions and a 6th-order compact scheme [5] in y direction. The velocity components are discretized as follows so that the boundary conditions are satisfied:

$$\begin{aligned} u(x, y, z) &= \sum u_{mn}(y) \cos(k_m x) \sin(k_n z) \\ v(x, y, z) &= \sum v_{mn}(y) \sin(k_m x) \sin(k_n z) \\ w(x, y, z) &= \sum w_{mn}(y) \sin(k_m x) \cos(k_n z) \end{aligned} \quad (4)$$

In order to remove the numerical instability due to the nonlinear terms, the 2/3-rule is applied for the horizontal directions

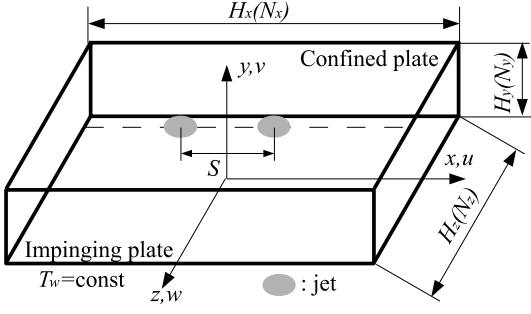


Figure 1: Coordinate system and computational domain

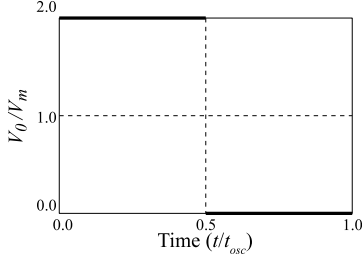


Figure 2: Intermittent control

and an implicit filtering for the wall-normal direction is conducted with 6th order compact scheme. For the time advancement, third order Adams-Bashforth method is used. The well-known MAC method is employed for pressure-velocity coupling, which results in a Poisson equation for the pressure. After the Poisson equation is expanded with sine series in x and z directions, the independent differential equations are obtained for each wave number and then are discretized with sixth order compact scheme. Finally, the penta-diagonal matrix is deduced for each wave number. In the present simulation code, these matrices are solved using the LU Decomposition method. When vortical structures approach the side boundary of impinging wall, relatively strong low-pressure regions being formed by vortical structures do not meet the pressure boundary condition, i.e., $p = 0$. In the present simulation, since the spectral method is used, the occurrence of this discrepancy at the side boundary induces the unphysical numerical oscillation in the whole flow field. Thus the vortical motions should be artificially reduced near the boundary. In the present simulation, the idea of a fringe (buffer) region [8] is introduced around the outflow boundary in order to reduce the perturbation using an appropriate external force.

Calculation Conditions

The inlet velocity distribution is assumed to be a top-hat type, which is given as follows:

$$V_{in}(r) = \frac{V_0}{2} - \frac{V_0}{2} \tanh \left[\frac{1}{4} \frac{R}{\theta_0} \left(\frac{r}{R} - \frac{R}{r} \right) \right] \quad (5)$$

where V_0 is the center velocity. θ_0 denotes the initial momentum thickness $R (= D/2)$ is a radius of an inlet jet. This inlet velocity profile is selected by referring to the literature [10]. ($R/\theta_0 = 20$). Figure 1 shows the computational volume and coordinate systems. In the present simulations, the distance to the impinging wall (plate), H is $H/D = 4$. Computational conditions such as the size of computational domain, the grid number, the Reynolds number and the Prandtl number is $(H_x, H_y, H_z) = (24D, 4D, 24D)$, $(N_x, N_y, N_z) = (128, 100, 128)$, $\text{Re} = 1500$ and $\text{Pr} = 0.71$, respectively. The grid spacing of wall-normal direc-

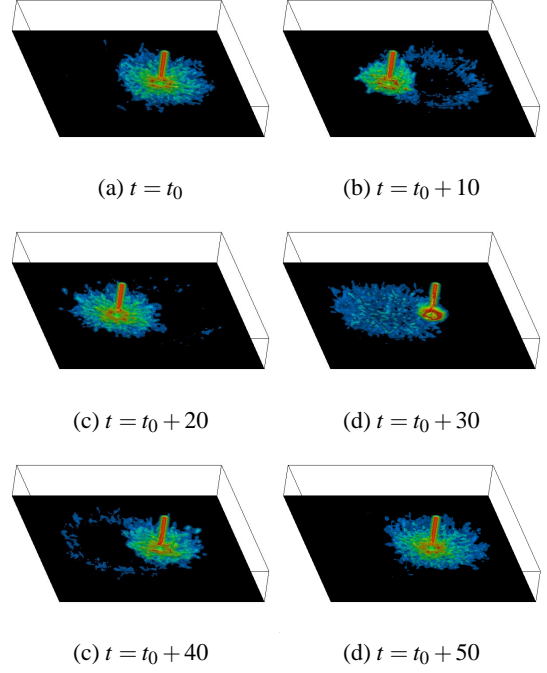


Figure 3: Contour of instantaneous velocity magnitude ($t_{osc} = 50, \delta = \pi$).

tion is densely populated near wall region. The inflow temperature, T_0 and the ambient temperature, T_a are assumed to be higher than the wall temperature, T_w , i.e., $T_0 = T_a > T_w$. In the present study, the boundary surface normal to the y direction excluding the jet inflow section is a wall surface. The separation between jet-jet, S is set to $S/D = 5.0$. Figure 2 shows inflow conditions in intermittently controlled case ($V_0 = 2V_m$). With reference to Xu, et al. [8, 9], jet issues in half of the period of intermittent control, in the remaining half period, the jet does not issue; the inflow velocity V_0 is set to $2V_m$ so that the time-averaged flow rate become as same as that of the uncontrolled jet. As control parameters, both the period of intermittent control, t_{osc} and the phase difference between two jets δ are varied as $t_{osc} = 5, 20, 50$ and $\delta = \pi/4, \pi/2, \pi$, respectively.

Results and Discussion

Flow Structure

In order to observe the state of the flow field under intermittent control, the 3D contours of instantaneous velocity magnitude are sequentially arranged by about 1/4 period of intermittent control in the case of $t_{osc} = 50, \delta = \pi$ in figure 3. In figure 3 (a), the jet located right side impinges on the wall and another jet does not issue. In figure 3(b), because of $\delta = \pi$ the left side jet only issues and impinges to the impinging wall. In figure 3(c) and (d), alternately each jet issues with a delay of the half period as well as figure 3 (a) and (b). In this way, it can be seen that the intermittent control with a phase difference between two jets reproduces intermittently impingement.

Figure 4 shows the contours of the time-averaged velocity magnitude on the $x - y$ plane through each jet center. Irrespective of the control parameter, the time-averaged result demonstrates that the jets impinge perpendicular to the impinging wall, and that the stagnation region is formed at the impingement points on the impinging wall. On the other hand, depending on the control parameter, the different feature appears: in figure 4 (a),

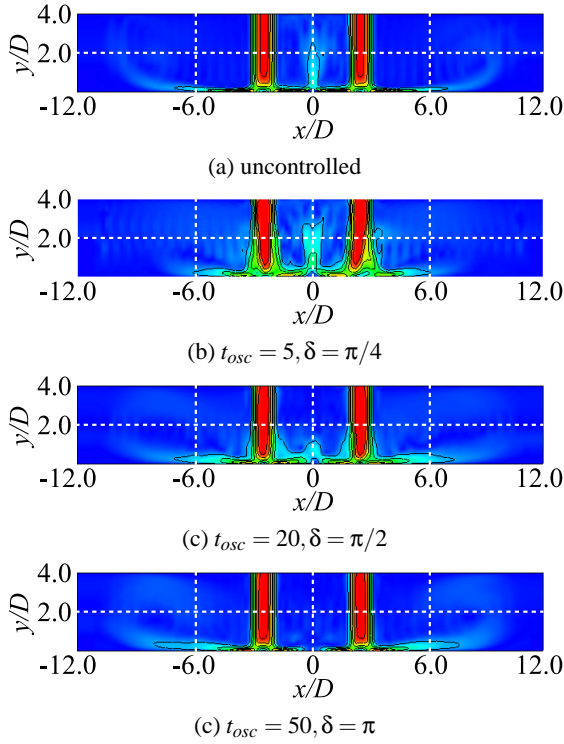


Figure 4: Contour of mean velocity magnitude

it can be seen that the up-wash flow between the two jets is formed due to the collision of the wall jets; in figure 4(b) since the both short intermittent period and the small phase difference induce frequently the occurrence of alternately issuing and enhances mutual interaction between two jets, unfortunately, stronger up-wash flow is formed; from figure 4 (c) and (d) a relatively long period and large phase difference induce the suppression of occurrence of up-wash flow, i.e., one jet impinges on the impinging wall without being affected by another jet flow. The wall-normal velocity distribution along x direction at $y/D = 2$ is shown in figure 5. In the figure, the positive velocity indicates the existence of up-wash flow. As shown in this figure, for a short period of $t_{osc} = 5$ including the phase difference $\delta = \pi/4$, $\pi/2$ and π and uncontrolled case, up-wash flow is formed between jets, while $t_{osc} = 20$ and 50 up-wash flow is reduced, suggesting that the intermittent control contributes to the reduction of up-wash flow. In addition, the wall-normal velocity at $(x, y, z) = (0, 2D, 0)$ is plotted in figure 6. The tendency of intermittent control is definitely observed: longer period and larger phase difference contributes to the reduction of up-wash flow

Heat transfer characteristics

The contour of the time-averaged local Nusselt number on the impinging wall is shown in figure 7 to demonstrate the HTP of the intermittently controlled MIJ. In the figure, high HTP appears around the impingement points of each jet regardless of the control conditions. Also, it can be seen that the basic heat transfer characteristics of impinging jet occur: as increasing distance from the impingement points, the HTP sharply decreases and that in the uncontrolled case, the HTP between two jets ($x = z = 0$) is deteriorated due to the interaction between the jets. Figure 8 shows the Nu number distribution along x direction. As well as Nu contour of figure 7, it can be confirmed that in all cases high HTP around impinging position appear and non-uniformity remains even in the intermittent control. Also, it re-confirmed for the uncontrolled case, the low HPT between jets and that for controlled cases HPT between jets is obviously im-

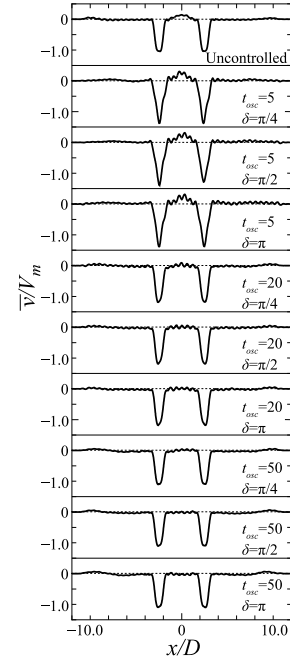


Figure 5: Distribution of mean wall-normal velocity on y -axis

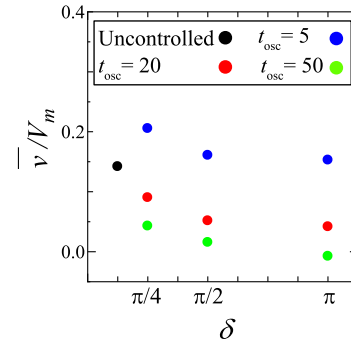


Figure 6: Mean wall-normal velocity on the y -axis at $y/D = 2.0$

proved.

The distribution of integrated Nusselt number on the impinging wall, Nu_{sum} is shown in figure 9. Nu_{sum} is defined as follow:

$$Nu_{sum}(r) = 2\pi \int_0^r Nur dr \quad (6)$$

where r is the distance from the center of the wall surface ($x = z = 0$). In the figure, to compare the uncontrolled case Nu_{sum} is divided by that of the uncontrolled case. As can be seen, at the any distance the HTP of the controlled jet is superior to that of uncontrolled jet; in all cases, the total heat transfer calculated at $r/D = 10.0$ is about $10 \sim 30\%$ higher than the uncontrolled case. In particular, the characteristics of HTP changes depending on the control parameter: paying attention to $r/D = 0$ (between two jets), the maximum value of HTP between two jets is markedly improved under the condition of the long period and the large phase difference; further looking at $2.0 < r/D < 6.0$ (range including the impingement points), the short period is superior to that of the long period.

Conclusion

In this present study, in order to elucidate the flow and heat char-

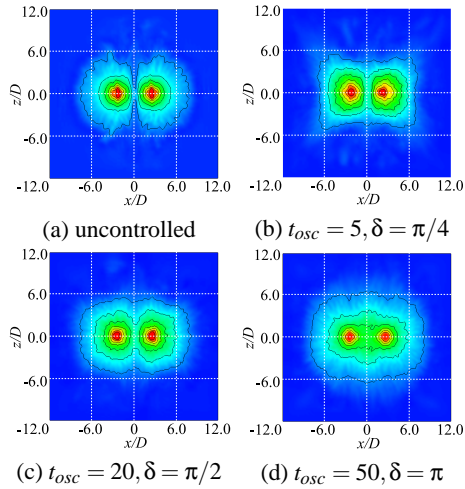


Figure 7: Contour of local Nusselt number

acteristics of intermittently controlled multiple impinging jets, we conduct the DNS of intermittently controlled two impinging jets arranged at an inflow of flow field. From the analysis of the flow structure, it reveals that the intermittent control suppresses the up-wash flow occurring between the jets; from the analysis of the heat transfer characteristics, the intermittent control is fairly capable of improving the heat transfer performance compared to that of the uncontrolled case, in particular, the total heat transfer of all cases is improved about 10 ~30% higher than that of the uncontrolled case.

References

[1] Farahani, S. D., Bijarchi, M. A., Kowsary, F. and Ashjaee, M., Optimization arrangement of two pulsating impingement slot jets for achieving heat transfer coefficient uniformity, *J. Heat Transfer*, **138**-10, 2016, 102001 (13 pages).

[2] Geers, L.F. G., Hanjalić, K., and Tummers, M. J. D., Wall imprint of turbulent structures and heat transfer in multiple impinging jet arrays, *J. Fluid Mech.*, **546**, 2006, 255-284.

[3] Hofmann, H. M., Luminita, D. Movileanu, D. L., Kind, M. and Martin, H., Influence of a pulsation on heat transfer and flow structure in submerged impinging jets, *Int. J. Heat and Mass Transfer*, **50**, 2007, 3638-3648.

[4] Kataoka, K., Impingement heat transfer augmentation due to large scale eddies, *In Heat Transfer 1990, Proc. 9th Intl Heat Transfer Conf.*, **1**, 1990, .255-273.

[5] Lele, S. K., Compact finite difference schemes with spectral-like resolution, *J. Comp. Phys.*, **103**, 1992, 16-42.

[6] Mladin, E. C. and D.A. Zumbrennen, D. A., Local convective heat transfer to submerged pulsating jets, *Int. J. Heat and Mass Transf.* **40**-14, 1997, 3305-3321.

[7] Mohammadpour, J., Zolfagharian, M. M., Mujumdar, A. S., Zargarabadi, M. R. and Abdulhazadeh, M., Heat transfer under composite arrangement of pulsed and steady turbulent submerged multiple jets impinging on a flat surface, *Int. J. Thermal Sciences*, **86**, 2014, 139-147.

[8] Nordstrom, J., Nordin, N., and Henningson, D. S., The fringe region technique and the Fourier method used in the direct numerical simulation of spatially evolving viscous flows, *SIAM J. Sci. Comp.*, **20**-4, 1999, 1365-1393.

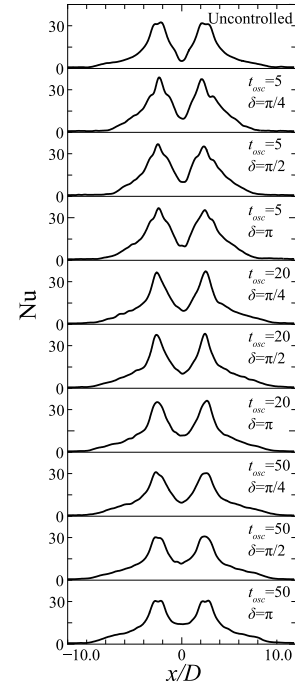


Figure 8: x-directional distribution of local Nusselt number at $z = 0$

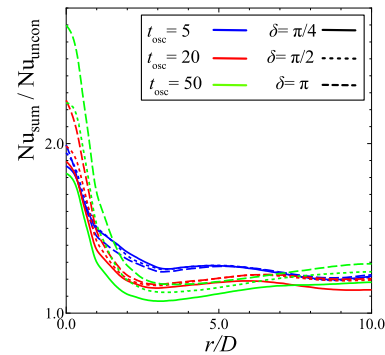


Figure 9: Distribution of $Nu_{sum}/Nu_{uncontrolled}$

[9] Sailor, D. J., Rohli, J. and Fu, Q., Effect of variable duty cycle flow pulsations on heat transfer enhancement for an impinging air jet, *Int. J. Heat and Fluid Flow*, **20**-6, 1999, 574-580.

[10] Silva, C. B. and Metais, O., Vortex control of bifurcating jets: A numerical study, *Phys. Fluids*, **14**, 2002, 3798-3819.

[11] Viskanta, R., Heat transfer to impinging isothermal gas and flame jets, *Exp. Therm. Fluid Sci.*, **6**, 1993, 111-134.

[12] Weigand, B. and Spring, S., Multiple jet impingement - a review, *Heat Transfer Res.*, **42**-2, 2011, 101-142.

[13] Xu, P. Yu, B., Qiu, Q., Poh, H. J. and Mujumdar, A. S., Turbulent impinging jet heat transfer enhancement due to intermittent pulsation', *Int. J. Thermal Sciences*, **49**, 2010, 1247-1252

[14] Xu, P., Qiu, S., Zhou, M. Y., Qiao, X. and Mujumdar, A. S., A study on the heat and mass transfer properties of multiple pulsating impinging jets, *Int. Commun. in Heat and Mass Transfer*, **39**, 2012, 378-382.